inconsistencies resolved as needed to provide an accurate technical basis for corrective action design.

FERENCES

Driscoll, F.G., *Ground Water and Wells*, St. Paul, Johnson Division, 1986.

U.S. Environmental Protection Agency, *Test Methods for Evaluating Solid Waste*, SW-846, Volumes 1A, 1B, 1C: Laboratory Manual, Volume 2: Field Manual, 3rd Ed., NTIS No. PB88239223. Washington, DC, U.S. Environmental Protection Agency, 1986.

U. S. Environmental Protection Agency, *Laboratory Data Validation, Functional Guidelines for Evaluating Inorganic Analyses*, Data Review Workshop, February, Hazardous Site Evaluation Division, U.S. EPA, Contract No. 68-01-7443, 1989a.

U.S. Environmental Protection Agency, *Laboratory Data Validation, Functional Guidelines for Evaluating Organic Analyses*, USEPA Data Review Workshop, Hazardous Site Evaluation Division, U.S. EPA, November 1988.

Heath, R.C., *Basic Ground Water Hydrology*, U.S.G.S. Water Supply Paper 2220, U.S. Government Printing Office, p. 84, 1983.

Hunt, Royrf E., *Geotechnical Engineering Investigation Manual*, New York, McGraw-Hill, 1984.

Keys, W.S. and L.M. MacCary, *Application of Borehole Geophysics to Water Resources Investigations*, Washington, U.S. Government Printing Office, 1971.

Scalf, M.R., J.F. McNabb, W.J. Dunlap, R.L. Cosby, J. Fryberger, *Manual of Ground Water Sampling Procedures*, Worthington, Ohio, NWWA, 1981.

Statistical Analysis of Ground Water Monitoring Data at RCRA Facilities—Interim Final Guidance, February, EPA/530/SW-89/026, NTIS No. PB89151047, U.S. EPA, 1989b.

Tearpock, D.J. and R.E. Bischke, *Applied Subsurface Geologic Mapping*, Englewood Cliffs, NJ, Prentice-Hall, p. 648, 1991.

Zohdy, A.A.R., G.P. Eaton, and D.R. Maybey, *Application of Surface Geophysics to Ground Water Investigations*, U.S. Government Printing Office, 1984.

CHAPTER 6

CONTAMINANT TRANSPORT MECHANISMS

6.1 INTRODUCTION

This chapter explores transport concepts relating to the migration and fate of contaminants from hazardous waste sites dissolved in ground water. The discussion will include case studies with applications for environmental engineers, hydrologists, hydrogeologists, and others in the ground water area. The approach considers the advective and dispersive transport of solutes dissolved in ground water, which may undergo simple first order decay or linear adsorption. Much effort has been devoted to solving the governing partial differential equations over the past two decades. Both one-dimensional (soil column) and two-dimensional (landfill plume) problems have generally been addressed. Mathematical derivations of the governing mass transport equations are reviewed in Section 6.4, and have been presented earlier by Ogata (1970), Bear (1972, 1979), and Freeze and Cherry (1979). This chapter deals primarily

with analytical and semi-analytical solutions, while Chapter 10 presents numerical approaches in detail.

Several recent reviews of solute transport modeling have been written, such as those by Mercer and Faust (1981), Anderson and Woessner (1992) and Zheng and Bennett (1995). Freeze and Cherry (1979) in their classic text offer clear descriptions of many transport mechanisms and derive many of the governing transport equations. Domenico and Schwartz (1998) present a number of analytical equations and solutions in their text on physical and chemical hydrogeology.

The concepts presented in this chapter serve as a synthesis of existing theory highlighted by examples and case studies for understanding and predicting migration and transport of solutes in ground water from hazardous waste sources. The main transport processes of concern in ground water include advection, diffusion, dispersion, adsorption, biodegradation and chemical reaction. Advection is the movement of contaminants along with flowing ground water at the seepage velocity in porous media. Diffusion is a molecular mass transport process in which solutes move from areas of higher concentration to areas of lower concentration. Dispersion is a mixing process caused by velocity variations in the porous media. Dispersion causes sharp fronts to spread out and results in the dilution of the solute at the advancing edge of the contaminant front. Adsorption, the partitioning of organic contaminants from the soluble phase onto the soil matrix, is covered in detail in Chapter 7. Aerobic biodegradation represents the transformation of certain organics to simple CO_2 and water in the presence of microbes in the subsurface. Biodegradation kinetics and other chemical reactions in ground water are covered in Chapter 7 and biodegradation modeling in Chapter 8. Transport mechanisms in the unsaturated or vadose zone are described in Chapter 9.

Nonaqueous phase liquids (NAPLs) are hydrocarbons that are slightly soluble in water, and can create major sources of long-term contamination in the subsurface. NAPLs are defined as separate phase products that are either lighter than water (LNAPL), such as normal gasoline, which can float above the water table, or denser than water (DNAPL), such as chlorinate solvents. Examples include PCE, TCE, and DCE, solvents which are denser than water and can sink to the bottom of an aquifer, or be held up by clay lenses and cause contamination problems for many years. NAPL formation and transport mechanisms are discussed in Chapter 11.

Advection, diffusion, dispersion, adsorption, and biodegradation have been analyzed in some detail under both laboratory and field conditions. Soil columns have been set up in the laboratory and loaded with numerous organic compounds similar to those found at hazardous waste sites. Dispersion coefficients, and rates of adsorption (retardation) and biodegradation have been evaluated with some success in these columns. Figure 6.1 shows the typical response (breakthrough curve) of a soil column loaded with a tracer or organic at one end and monitored at the outlet as a function of time.

Field efforts in the mid 1980s and early 1990's attempted to quantify dispersion, adsorption, and biodegradation mechanisms. One of the most successful field sites for tracer studies has been the Borden landfill site in Canada, which resulted in a series of classic papers on dispersion and adsorption processes measured during a multi-year field experiment

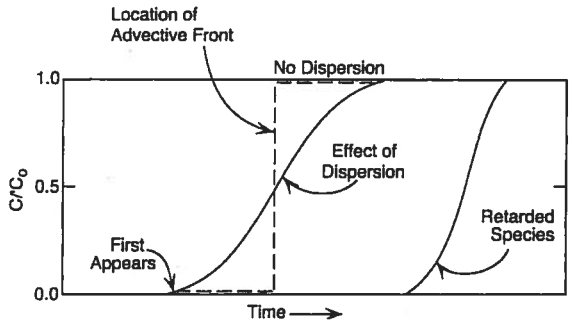

Figure 6.1 Breakthrough curves in 1-D showing effects of dispersion and retardation.

(Mackay et al., 1986; Roberts et al., 1986). LeBlanc et al. (1991) describe a natural gradient tracer experiment performed at Otis Air Base on Cape Cod, Massachusetts where more than 30,000 samples were analyzed over a two-year period. Detailed comparisons with the results from the Borden landfill were made (Section 6.10).

Borden and Bedient (1986), Rifai et al. (1988), and Barker et al. (1987) reported some success in measuring and modeling the biodegradation of contaminant plumes associated with naphthalene and BTEX in ground water. Several of these field projects are described in detail in later sections of the text.

The incorporation of the above transport mechanisms into ground water models for prediction and evaluation of waste sites h as been described in many references over the past two decades. Some of the earliest efforts are presented in Bear (1972), Bredehoeft and Pinder (1973), Fried (1975), Anderson (1979), Bear (1979), and Freeze and Cherry (1979). More recently, Domenico and Schwartz (1998), Anderson and Woessner (1992), and Zheng and Bennett (1995) provide discussion of some of the more complex flow and transport issues facing the ground water modeler.

6.2 ADVECTION PROCESS

Advection represents the movement of a contaminant with the flowing ground water according to the seepage velocity in the pore space, which was defined in Eq. (2.5).

$$v_x = -\frac{K}{n}\frac{dh}{dL}$$

It is important to realize that seepage velocity equals the average linear velocity of a contaminant in porous media, and is the correct velocity for use in governing solute transport equations. As defined earlier, the average linear velocity, v_x, equals the Darcy velocity divided by effective porosity, n, associated with the pore space through which water can actually flow. The average linear velocity is less than the microscopic velocities of water molecules moving along individual flowpaths, due to tortuosity. The one dimensional (1-D) mass flux (F_x) due to advection equals the product of water flow and concentration (C) of solute, or $F_x = v_x nC$.

There are certain cases in the field where an advective model provides a useful estimate of contaminant transport. Some models include the concept of arrival time by integration along known streamlines (Nelson, 1977). Streamline models are used to solve for arrival times of particles that move along the streamlines at specified velocities, usually in a two dimensional (2-D) flow net. Others have set up an induced flow field through injection or pumping and evaluated breakthrough curves by numerical integration along flow lines. Dispersion is not directly considered in these models, but results from the variation of velocity and arrival times in the flow field (Charbeneau, 1981, 1982). In cases where pumping of ground water is dominating the flow field, it may be useful to neglect dispersion processes without loss of accuracy. In Chapter 10, it will be shown how advection is treated numerically by particle mover models, which represent the velocity of individual particles moving according to the local velocity field in the x or y direction.

DIFFUSION AND DISPERSION PROCESSES

Diffusion is a molecular-scale process, which causes spreading due to concentration gradients and random motion. Diffusion causes a solute in water to move from an area of higher concentration to an area of lower concentration. Diffusive transport can occur in the absence of velocity. Mass transport in the subsurface due to diffusion in 1-D can be described by Fick's first law of diffusion,

$$f_x = -D_d \frac{\partial C}{\partial x} \tag{6.1}$$

where

f_x = mass flux [M/L²/T]
D_d = diffusion coefficient [L²/T]
dC/d_x = concentration gradient [M/L³/L]

Diffusion is usually only a factor in the case of very low velocities such as in a tight soil or clay liner, or in the case of mass transport involving very long time periods. Typical values of D_d are relatively constant and range from 1×10^{-9} to 2×10^{-9} m²/sec at 25°C. Typical

dispersion coefficients in ground water are several orders of magnitude larger and tend to dominate the spreading process when velocities are present.

A soil column similar to the one used by Darcy can be used to introduce the concept of advective-dispersive transport. The column is loaded continuously with tracer at relative concentration of $C/C_0 = 1$ across the entire cross section. Figure 6.1 shows the resulting concentration versus time response measured at $x = L$, called the breakthrough curve. The step function loading is begun at $t = 0$, and the breakthrough curve develops due to dispersion processes which create a zone of mixing between the displacing fluid and the fluid being displaced. The advective front (center of mass) moves at the average linear velocity (or seepage velocity) and $C/C_0 = 0.5$ at that point as shown in Figure 6.1. Velocity variations within the soil column cause some of the mass to leave the column in advance of the advective front and some lags behind, producing a dispersed breakthrough curve in the direction of flow. The size of the mixing zone increases as the advective front moves farther from the source, but at some distance behind the advective front, the source concentration C_0 is encountered, and it remains at steady state in this region. If there were no dispersion, the shape of the breakthrough curve would be identical to the step input function.

Dispersion is caused by heterogeneities in the medium that create variations in flow velocities and flow paths. These variations can occur due to friction within a single pore channel, due to velocity differences from one channel to another, or due to variable path lengths. Laboratory column studies indicate dispersion is a function of average linear velocity and a factor called dispersivity, α. Dispersivity in a soil column is on the order of centimeters, while values in field studies may be on the order of one to thousands of meters. Figure 6.2 shows the factors causing longitudinal dispersion (D_x) of a contaminant in the porous media.

Mass transport due to dispersion can also occur normal to the direction of flow. This transverse dispersion, D_y, is caused by diverging flowpaths in the porous media that cause mass to spread laterally from the main direction of flow. In most cases involving a two-dimensional plume of contamination, D_y is much less than D_x, and the shape of the plume tends to be elongated in the direction of flow.

Freeze and Cherry (1979) defined hydrodynamic dispersion as the process in which solutes spread out and are diluted compared to simple advection alone. It is defined as the sum of molecular diffusion and mechanical dispersion, where much dispersion is caused by local variations in velocity around some mean velocity of flow.

Dispersion in 2-D causes spreading in the longitudinal (x) and transverse (y) directions both ahead of and lateral to the advective front. Many typical contaminant plumes in ground water are represented by 2-D advective-dispersive mechanisms. Figure 6.3 depicts the normal shape of such a plume in 2-D compared to advection alone. Longitudinal dispersion causes spreading and decreases concentrations near the frontal portions of the

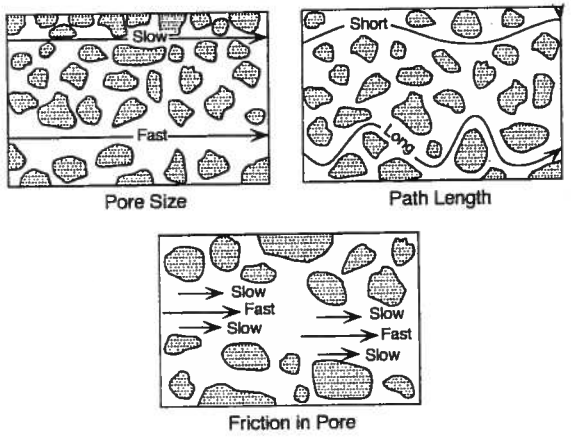

Figure 6.2 Factors causing longitudinal dispersion.

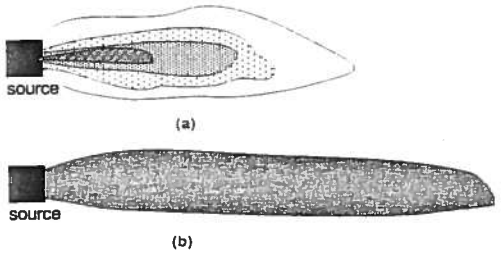

Figure 6.3 (a) Advection and dispersion. (b) Advection only.

plume. The main difference with the 1-D soil column results described above is that 2-D plumes have transverse spreading which reduces concentrations everywhere behind the advective front.

For the case of an instantaneous or pulse source (such as a sudden release or spill of contaminant into the subsurface), the variation in concentration with time and space is shown in Figure 6.4. The concentration distributions start out with sharp fronts and are smoothed out as the contaminant is diluted through dispersive mixing. The center of mass is advected at the average linear velocity. Concentrations can be described by

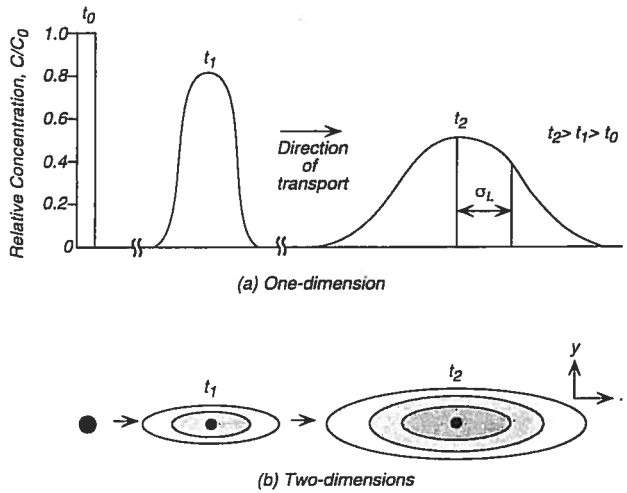

Figure 6.4 Instantaneous (Pulse) source. The shapes can be represented by Gaussian (Normal) distributions.

Gaussian or normal distributions in 1-D, 2-D, or 3-D geometries. Equations for prediction of pulse source concentrations as a function of space and time are presented in Sections 6.5 and 6.7. From the characteristics of the normal curves in Figure 6.4, one can show that dispersion coefficients can be related to the variance of the distributions, $D_x = \sigma_x^2/2t$ and $D_y = \sigma_y^2/2t$. Thus, by measuring the spread or variance in a plume, one can estimate a value for D_x and D_y at a field site. Dispersion is discussed in more detail in Sections 6.9 and 6.10.

6.4 MASS TRANSPORT EQUATIONS

Dispersive flux in a flow field with average linear velocity components v_x and v_y can be written in terms of the statistical fluctuations of velocity about the average, v_{x*} and v_{y*}. For the case of a uniform flow field where $v_x = \bar{v}_x$ a constant, and $v_y = 0$, dispersive flux is assumed proportional to the concentration gradient in the x direction:

$$f_{x*} = nCv_{x*} = -nD_x \frac{\partial C}{\partial x} \tag{6.2}$$

where D_x is the longitudinal dispersion coefficient, n is effective porosity and C is concentration of contaminant tracer. Similarly, the dispersive flux f_{y*} is assumed proportional to the concentration gradient in the y direction:

$$f_{y*} = nCv_{y*} = -nD_y \frac{\partial C}{\partial y} \tag{6.3}$$

For a simple uniform flow field with average linear velocity $\bar{v}_x$

$$D_x = \alpha_x \bar{v}_x \tag{6.4}$$

$$D_y = \alpha_y \bar{v}_x \tag{6.5}$$

where α_x and α_y are the longitudinal and transverse dispersivities, respectively.

Dispersivity values have usually been set constant in transport models, but studies by Smith and Schwartz (1980) and Gelhar et al. (1979) indicate that dispersivity depends on the distribution of heterogeneities and the scale of the field problem. Many investigators during the decade of the eighties worked on the complex problem of estimating dispersivity from field tracer studies and pump tests, and both statistical and deterministic models have been postulated (Anderson, 1979; Freeze and Cherry, 1979; Mackay et al., 1986; Gelhar and Axness, 1983; Freyberg, 1986; Dagan, 1986, 1987, 1988; Neuman et al., 1987).

It should be noted that dispersion coefficients become more complex in a nonuniform flow field characterized by v_x and v_y. The dispersion coefficient relates the mass flux vector to the gradient of concentration and can be represented as a second rank tensor (Bear, 1979). Through careful definition of the coordinate system, relationships can be developed between D_x, D_y, and D_z and the components of the tensor $[D]$ (Wang and Anderson, 1982).

6.4.1 Derivation of the Advection Dispersion Equation for Solute Transport

The equation governing transport in ground water is a statement of the law of conservation of mass. The derivation is based on those of Ogata (1970) and Bear (1972) and is presented in Freeze and Cherry (1979). It will be assumed that the porous medium is homogeneous and isotropic, and saturated; it is further assumed that the flow is steady-state and that Darcy's law applies. The flow is described by the average linear velocity or seepage velocity, which transports the dissolved substance by advection. If advection were the only transport mechanism operating, conservative solutes would move according to plug flow concepts. In reality, there is an additional mixing process, hydrodynamic dispersion, which is caused by velocity variations within each pore channel and from one channel to another. Hydrodynamic dispersion is used to account for the additional transport (spreading) caused by the fluctuations in the velocity field.

To establish the mathematical statement of the conservation of mass, the solute flux into and out of a representative elemental volume in the porous medium will be considered (Figure 6.5). In Cartesian coordinates the specific discharge v has components (v_x, v_y, v_z) and the average linear velocity $\bar{v} = v/n$ has components ($\bar{v}_x$, $\bar{v}_y$, $\bar{v}_z$). The rate of advective transport is equal to $\bar{v}$. The concentration of the solute C is defined as the mass of solute per unit volume of solution. The mass of solute per unit volume of porous media is therefore nC. For a homogeneous medium, the effective porosity n is a constant, and $\partial(nC)/\partial x = n\ \partial C/\partial x$. The mass of solute transported in the x-direction by the two mechanisms of solute transport can be represented as

$$\text{transport by advection} = \bar{v}_x nC\, dA \tag{6.6}$$

$$\text{transport by dispersion} = nD_x \frac{\partial C}{\partial x} dA$$

where D_x is the hydrodynamic dispersion coefficient in the x-direction and dA is the elemental cross-sectional area of the cubic element. The dispersion coefficient D_x is related to the dispersivity αx and the diffusion coefficient D_d by:

$$D_x = \alpha_x \bar{v}_x + D_d \tag{6.7}$$

The form of the dispersive component embodied in Eq. (6.6) is analogous to Fick's first law.

If F_x represents the total mass of solute per unit cross-sectional area transported in the x direction per unit time, then

$$F_x = \bar{v}_x nC - nD_x \frac{\partial C}{\partial x} \tag{6.8}$$

The negative sign before the dispersive term indicates that the contaminant moves toward the area of lower concentration. Similarly, expressions for flux in the other two directions can be written

$$F_y = \bar{v}_y nC - nD_y \frac{\partial C}{\partial y} \tag{6.9}$$

$$F_z = \bar{v}_z nC - nD_z \frac{\partial C}{\partial z} \tag{6.10}$$

The total amount of solute entering the fluid element (Figure 6.5) is

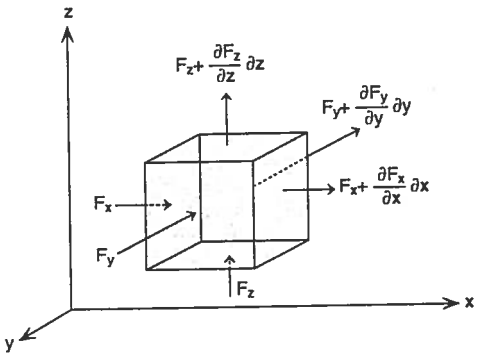

Figure 6.5 Mass balance in a cubic element in space.

$$F_x dzdy + F_y dzdx + F_z dxdy$$

The total amount leaving the representative fluid element is

$$\left(F_x + \frac{\partial F_x}{\partial x}dx\right)dzdy + \left(F_y + \frac{\partial F_y}{\partial y}dy\right)dzdx + \left(F_z + \frac{\partial F_z}{\partial z}dz\right)dxdy$$

The difference in the amount entering and leaving the fluid element is

$$\left(\frac{\partial F_x}{\partial x} + \frac{\partial F_y}{\partial y} + \frac{\partial F_z}{\partial z}\right)dxdydz$$

Because the dissolved tracer is assumed to be conservative (nonreactive), the difference between the flux into the element and the flux out of the element equals the amount of dissolved substance accumulated in the element. The rate of mass change in the element can be represented by

$$-n\frac{\partial C}{\partial t}dxdydz$$

The complete conservation of mass expression, therefore, becomes

$$\frac{\partial F_x}{\partial x} + \frac{\partial F_y}{\partial y} + \frac{\partial F_z}{\partial z} = -n\frac{\partial C}{\partial t} \tag{6.11}$$

Substitution of expressions for F_x, F_y, and F_z into (6.11) and cancellation of n from both sides of the equation yield:

$$\left[\frac{\partial}{\partial x}\left(D_x\frac{\partial C}{\partial x}\right) + \frac{\partial}{\partial y}\left(D_y\frac{\partial C}{\partial y}\right) + \frac{\partial}{\partial z}\left(D_z\frac{\partial C}{\partial z}\right)\right]$$

$$-\left[\frac{\partial}{\partial x}(\bar{v}_x C) + \frac{\partial}{\partial y}(\bar{v}_y C) + \frac{\partial}{\partial z}(\bar{v}_z C)\right] = \frac{\partial C}{\partial t} \tag{6.12}$$

In a homogeneous medium in which the velocity is steady and uniform (i.e., if it does not vary through time or space), and dispersion coefficients D_x, D_y, and D_z do not vary through space, (but $D_x \neq D_y \neq D_z$, in general), Eq. (6.12) becomes

$$\left[D_x\frac{\partial^2 C}{\partial x^2} + D_y\frac{\partial^2 C}{\partial y^2} + D_z\frac{\partial^2 C}{\partial z^2}\right] - \left[\bar{v}_x\frac{\partial C}{\partial x} + \bar{v}_y\frac{\partial C}{\partial y} + \bar{v}_z\frac{\partial C}{\partial z}\right] = \frac{\partial C}{\partial t} \tag{6.13}$$

In two dimensions, the governing equation for a one-dimensional velocity becomes

$$\left[D_x\frac{\partial^2 C}{\partial x^2} + D_y\frac{\partial^2 C}{\partial y^2}\right] - \left[\bar{v}_x\frac{\partial C}{\partial x}\right] = \frac{\partial C}{\partial t} \tag{6.14}$$

In one dimension, such as for a soil column, the governing equation reduces to the familiar advective-dispersion equation, which can be solved using Laplace transforms,

$$D_x\frac{\partial^2 C}{\partial x^2} - \bar{v}_x\frac{\partial C}{\partial x} = \frac{\partial C}{\partial t} \tag{6.15}$$

A number of analytical solutions exist for Eqs. (6.13), (6.14) and (6.15) under various simplifying assumptions and some of these are presented in Section 6.5.

ONE-DIMENSIONAL MODELS

The governing mass transport Eq. (6.13) is difficult to solve in field cases of practical interest due to boundary irregularities and variations in aquifer characteristics, so numerical methods must generally be employed. There are, however, a limited number of relatively simple, 1-D problems for which analytical solutions exist. Several of these cases are presented below in order to gain insights into the effect of advection, dispersion, and adsorption on the overall patterns produced.

The simplifying assumptions include the following: (1) the tracer is ideal, with constant density and viscosity; (2) the fluid is incompressible; (3) the medium is homogeneous and isotropic; and (4) only saturated flow is considered. For the case of a nonreactive tracer in 1-D flow in the $+x$ direction, Eq. (6.15) applies.

$$D_x \frac{\partial^2 C}{\partial x^2} - v_x \frac{\partial C}{\partial x} = \frac{\partial C}{\partial t} \tag{6.16}$$

where D_x = coefficient of hydrodynamic dispersion and v_x = average seepage velocity. Note that the bar over the velocity terms is dropped for convenience.

Several different solutions can be derived for Eq. (6.16) depending on initial and boundary conditions and whether the tracer input is a slug input or a continuous release (Figures 6.1 and 6.4a). Initial conditions ($t = 0$) in a soil column are usually set to zero ($C(x,0) = 0$) or to some constant background concentration. Boundary conditions must be specified at the two ends of the 1-D column. For a continuous source load at $x = 0$, the concentration is set to $C(0,t) = C_0$ for $t > 0$. The concentration at the other boundary, $x = \infty$ is set to zero $C(x, \infty) = 0$ for $t > 0$.

Case 6.1 Continuous Source in 1-D. For an infinite column with background concentration of zero and input tracer concentration C_0 at $-\infty \le x \le 0$ for $t \ge 0$, Bear (1961) solves the problem using the Laplace transform at $x = L$, length of the column:

$$\frac{C(x,t)}{C_0} = \frac{1}{2}\left(\operatorname{erfc}\left[\frac{L - v_x t}{2\sqrt{D_x t}}\right] + \exp\left(\frac{v_x L}{D_x}\right)\operatorname{erfc}\left[\frac{L + v_x t}{2\sqrt{D_x t}}\right]\right) \tag{6.17}$$

where erfc is the complementary error function, $\operatorname{erfc}(x) = 1 - \operatorname{erf}(x) = 1 - \left(2/\sqrt{\pi}\right)\int_0^x e^{-u^2}\,du$

The center of mass ($C/C_0 = 0.5$) of the breakthrough curve travels with the average linear velocity v_x and corresponds to the point where $x = v_x t$. Note that the second term on the right hand side of Eq. (6.17) can generally be neglected for most practical problems. The error function erf (β) and erfc(β) are tabulated in Table 6.1.

TABLE 6.1 Values of erf (β) and erfc (β) for positive values of β

β	erf (β)	erfc (β)
0	0	1.0
0.05	0.056372	0.943628
0.1	0.112463	0.887537
0.15	0.167996	0.832004
0.2	0.222703	0.777297
0.25	0.276326	0.723674
0.3	0.328627	0.671373
0.35	0.379382	0.620618
0.4	0.428392	0.571608
0.45	0.475482	0.524518
0.5	0.520500	0.479500
0.55	0.563323	0.436677
0.6	0.603856	0.396144
0.65	0.642029	0.357971
0.7	0.677801	0.322199
0.75	0.711156	0.288844
0.8	0.742101	0.257899
0.85	0.770668	0.229332
0.9	0.796908	0.203092
0.95	0.820891	0.179109
1.0	0.842701	0.157299
1.1	0.880205	0.119795
1.2	0.910314	0.089686
1.3	0.934008	0.065992
1.4	0.952285	0.047715
1.5	0.966105	0.033895
1.6	0.976348	0.023652
1.7	0.983790	0.016210
1.8	0.989091	0.010909
1.9	0.992790	0.007210
2	0.995322	0.004678
2.1	0.997021	0.002979
2.2	0.998137	0.001863
2.3	0.998857	0.001143
2.4	0.999311	0.000689
2.5	0.999593	0.000407
2.6	0.999764	0.000236
2.7	0.999866	0.000134
2.8	0.999925	0.000075
2.9	0.999959	0.000041
3	0.999978	0.000022

Source: Domenico and Schwartz, 1990

Case 6.2 Instantaneous Source in 1-D. The corresponding solution can be derived for the injection of a tracer pulse (instantaneous input) at $x = 0$ with background concentration equal to zero in the column. As the slug moves downstream with v_x in the $+x$ direction, it spreads out according to

$$C(x,t) = \frac{M}{(4\pi D_x t)^{1/2}} \exp\left[-\frac{(x - v_x t)^2}{4 D_x t}\right] \tag{6.18}$$

where M is the injected mass per unit cross-sectional area. Figure 6.4 shows the resulting Gaussian distribution of concentration for the instantaneous pulse source in one-dimension.

Plots comparing the shapes of Eqs. (6.17) and (6.18) are shown in Figures 6.1 and 6.4, respectively, at $x = L$ at the end of a soil column. The differences between instantaneous (spike) source and continuous source transport problems are obvious in 1-D. The continuous source produces a response or breakthrough curve, which starts at a low concentration and eventually levels off to the initial input concentration C_0 as a function of time. The spike source produces a normal or Gaussian distribution which continues to decrease in maximum concentration due to spreading out with time in the direction of flow. For the spike source, the amount of mass under each curve is identical if the tracer is conservative.

Case 6.3 Adsorption Effects. While there exist many reactions that can alter contaminant concentrations in ground water, adsorption onto the soil matrix appears to be one of the dominant mechanisms. Adsorption is covered in more detail in Chapter 7. The concept of the isotherm is used to relate the amount of contaminant adsorbed by the solids S to the concentration in solution, C. One of the most commonly used isotherms is the Freundlich isotherm,

$$S = K_d C^b \tag{6.19}$$

where S is the mass of solute adsorbed per unit bulk dry mass of porous media, K_d is the distribution coefficient, and b is an experimentally derived coefficient. If $b = 1$, Eq. (6.19) is known as the linear isotherm and is incorporated into the 1-D advective-dispersion equation in the following way:

$$D_x \frac{\partial^2 C}{\partial x^2} - v_x \frac{\partial C}{\partial x} - \frac{\rho_b}{n}\frac{\partial S}{\partial t} = \frac{\partial C}{\partial t} \tag{6.20}$$

where ρ_b is the bulk dry mass density, n is porosity, and

$$-\frac{\rho_b}{n}\frac{\partial S}{\partial t} = \frac{\rho_b}{n}\frac{dS}{dC}\frac{\partial C}{\partial t}$$

For the case of the linear isotherm, $(dS/dC) = K_d$, and

$$D_x \frac{\partial^2 C}{\partial x^2} - v_x \frac{\partial C}{\partial x} = \frac{\partial C}{\partial t}\left(1 + \frac{\rho_b}{n} K_d\right)$$

or finally,

$$\frac{D_x}{R}\frac{\partial^2 C}{\partial x^2} - \frac{v_x}{R}\frac{\partial C}{\partial x} = \frac{\partial C}{\partial t} \tag{6.21}$$

where $R = [1 + (\rho_b/n)\, K_d]$ = retardation factor, which has the effect of retarding the adsorbed species relative to the advective velocity of the ground water (Figure 6.1). The retardation factor is equivalent to the ratio of velocity of the sorbing contaminant and the ground water and ranges from one to several thousand.

The use of the distribution coefficient assumes that partitioning reactions between solute and soil are very fast relative to the rate of ground water flow. Thus, it is possible for nonequilibrium fronts to occur that appear to migrate faster than retarded fronts, which are at equilibrium. These complexities involve other rate-kinetic factors beyond the scope of simple models discussed in this chapter (see Chapter 7).

An interesting case study is that of a semi-infinite column where the column ($x > 0$) is initially at $C = 0$, and is connected to a contaminant source containing tracer at $C = C_0$ ($x = 0$). The tracer continuously moves down the column at seepage velocity v_x in the $+x$ direction. It is assumed that $C = 0$ at $x = \infty$. For the case of linear adsorption, Eq. (6.21) is used, where R = retardation factor ≥ 1 described earlier for adsorption. The solution in this case becomes (Bear, 1972)

$$C(x,t) = \frac{C_0}{2}\left[\operatorname{erfc}\left(\frac{Rx - v_x t}{2\sqrt{RD_x t}}\right) + \exp\left(\frac{v_x x}{D_x}\right)\operatorname{erfc}\left(\frac{Rx + v_x t}{2\sqrt{RD_x t}}\right)\right] \tag{6.22}$$

Ogata and Banks (1961) showed that the second term in Eq. (6.22) can be neglected where $D_x/v_x x < 0.002$; this condition produces an error of less than 3%. Equation (6.22) then reduces to a form similar to Eq. (6.17) with an adjustment for R.

Equation (6.17) or (6.22) can be used in laboratory studies to determine dispersion coefficients for nonreactive and adsorbing species. Retarded fronts can be derived from conservative fronts by adjusting v_x/R and D_x/R in 1-D. Typical values of R for organics often encountered in field sites range from 2 to 10 (Roberts et al. 1986). Larger values of D_x tend to spread out the fronts while large values of R tend to slow the velocity of the center of mass ($C/C_0 = 0.5$) and reduce D_x by a factor of $1/R$. Conceptually, in 1-D, these transport mechanisms are relatively well understood for laboratory scale experiments.

Case 6.4 Transport and 1-D with First Order Decay. One example of mass transport that includes a simple kinetic reaction is the first order decay of a solute. This could be caused by radioactive decay, biodegradation, or hydrolysis, and is generally repre-

sented in the transport equation by adding the term $-\lambda C$, where λ is the first order decay rate in units of t^{-1}. For example, Eq. (6.16) would become the following:

$$D_x \frac{\partial^2 C}{\partial x^2} - v_x \frac{\partial C}{\partial x} - \lambda C = \frac{\partial C}{\partial t} \tag{6.23}$$

The resulting solution to the equation for a pulse source is given by Eq. (6.18) but multiplied by the factor $e^{-\lambda t}$. In general, the effect of the decay coefficient is to reduce mass and concentration as a function of time. This concept is described in more detail for hydrolysis and biodegradation in Chapters 7 and 8.

Example 6.1. APPLICATION OF 1-D TRANSPORT EQUATION

a) An underground tank leaches an organic (benzene) continuously into a one-dimensional aquifer having a hydraulic conductivity of 2.15 m/day, an effective porosity of 0.1 and a hydraulic gradient of 0.04 m/m. Assuming an initial concentration of 1000 mg/L, and longitudinal dispersivity of 7.5 m, find the time taken for the contaminant concentration to reach 100 mg/L at $L = 750$ m. Neglect any other degradation processes.

Seepage velocity v_x is calculated from Darcy's Law:

$$v_x = \frac{K\Delta h / \Delta x}{n} = \frac{2.15 \times 0.04}{0.1} = 0.86 \text{ m/day}$$

$$D_x = \alpha_x v_x = 7.5 \times 0.86 = 6.45 \text{ m}^2\text{/day}$$

Using Eq. (6.17) and ignoring the second term,

$$C(L,t) = \frac{C_0}{2} \operatorname{erfc}\left(\frac{L - v_x t}{2\sqrt{D_x t}}\right)$$

$$100 = 500 \operatorname{erfc}\left(\frac{750 - 0.86t}{2\sqrt{6.45t}}\right)$$

$$\frac{750 - 0.86t}{2\sqrt{6.45t}} = 0.9064$$

By trial and error,

$$\boxed{t = 728 \text{ days} = 1.99 \text{ yr}}$$

b) One of the drums stored at the above site breaks and suddenly releases 1 kg of decaying Cs-137 (half life of 33 years) over the cross-section of flow, which is estimated to be 10 m^2. What is the concentration (in mg/m^3) at $L = 100$ m, 90 days later?

Solution. The decay rate is calculated:

$$\lambda = \frac{\ln 2}{(33 \times 365)} = 5.755 \times 10^{-5} \text{ day}^{-1}$$

Using Eq. (6.18) and incorporating radioactive decay,

$$C(x,t) = \left\{\frac{\mu}{\sqrt{4\pi D_x t}} \exp\left[-\frac{(x - v_x t)^2}{4 D_x t}\right]\right\} \exp(-\lambda t)$$

$$= \frac{10^6 \text{mg}/10\text{m}^2}{\sqrt{4\pi(6.45)(90)}} \exp\left\{-\frac{[100 - (0.86)(90)]^2}{4 \times 6.45 \times 90}\right\} \exp\left(-5.755 \times 10^{-5} \times 90\right)$$

$$\boxed{C(x,t) = 934.79 \text{mg/m}^3 \text{ or } 0.935 \text{ mg/L}}$$

6.6 GOVERNING FLOW AND TRANSPORT EQUATIONS

The differential equation for simulating ground water flow in two dimensions is usually written (see Eq. (2.26) and (2.28))

$$\frac{\partial}{\partial x}\left(T_x \frac{\partial h}{\partial x}\right) + \frac{\partial}{\partial y}\left(T_y \frac{\partial h}{\partial y}\right) = S \frac{\partial h}{\partial t} + W \tag{6.24}$$

where

$T_x = K_x b$ = transmissivity in the x direction [L^2/T]
$T = K_y b$ = transmissivity in the y direction [L^2/T]
b = aquifer thickness [L]
S = storage coefficient
W = source or sink term [L/T]
H = hydraulic head [L]

The governing flow equation in 2-D must be solved before the transport equation can be solved. Chapter 10 describes numerical methods that can be used to solve Eq. (6.24) for an

actual field site. The resulting head distribution $h\,(x, y)$ can then be used to determine gradients and seepage velocities in two dimensions.

The governing transport equation in 2-D is usually written

$$\frac{\partial}{\partial x}\left(D_x \frac{\partial C}{\partial x}\right) + \frac{\partial}{\partial y}\left(D_y \frac{\partial C}{\partial y}\right) - \frac{\partial}{\partial x}\left(Cv_x\right) - \frac{\partial}{\partial y}\left(Cv_y\right) - \frac{C_0 W}{nb} + \Sigma R_k = \frac{\partial C}{\partial t} \qquad (6.25)$$

where

C = concentration of solute [M/L^3]
v_x, v_y = seepage velocity [L/T] averaged in the vertical direction
D_x, D_y = coefficient of dispersion [L^2/T] in x and y directions
C_0 = solute concentration in source or sink fluid [M/L^3]
R_k = rate of addition or removal of solute (±) [M/L^{3}T]
N = effective porosity
W = source or sink term

Equation (6.25) can only be solved analytically under the most simplifying conditions where velocities are constant, dispersion coefficients are constant, and source terms are simple functions. There are difficulties in attempting to use the mass transport equation to describe an actual field site, since dispersivities in the x and y directions are difficult to estimate from tracer tests due to the presence of spatial heterogeneities and other reactions in the porous media. Estimation of hydraulic conductivity, and associated velocities, can be quite difficult due to the presence of field heterogeneities that are often unknown. The source or sink concentrations that drive the model are usually assumed constant in time, but may actually have varied significantly. A particularly serious problem appears to be the reaction term, which may represent adsorption, ion exchange, or biodegradation. The assumption of equilibrium conditions and the selection of rate coefficients are both subject to some error and may create prediction problems at many field sites. In addition, fuels and solvents can create nonaqueous phase liquids (NAPLs) in the subsurface, which are difficult to measure and can provide sources of soluble contaminants for years to come (Chapter 11).

Despite all the above mentioned problems, mass transport models still offer the most reliable approach to organization of field data, prediction of plume migration, and ultimate management of waste-disposal problems. While a complete 3-D scenario with all rate coefficients included will probably never be achieved, presently existing 1-D and 2-D solute transport models have much to offer in simplifying and providing insight into complex ground water problems. Chapter 10 presents numerical methods for the solution of 2-D and 3-D flow and solute transport problems.

6.7 ANALYTICAL METHODS

Two-dimensional analytical modeling is one of the most useful tools for analyzing and predicting solute transport in a field situation. This type of model is considerably more versatile than the 1-D models previously discussed. Horizontal 2-D modeling can be used where (1) no vertical velocity components exist, or (2) observation wells or monitoring points are fully screened and provide averaged data in 2-D for a relatively uniformly thick aquifer. Nonuniformities in the flow field may be due to variations in topography and permeability, or to natural or artificial sinks such as wells and springs, or to recharge points such as injection wells or leakage from lagoons. Probably the most common reason for using a horizontal 2-D analysis is that the monitoring wells are typically distributed about the horizontal plane. Most wells are fully penetrating, and therefore any samples collected represent an approximate vertical average in that portion of the aquifer.

Sampling in the vertical direction may be warranted where there are significant differences between the contaminant density and water density or where detailed information is available on vertical variations in aquifer hydraulic conductivity or porosity. Profile 2-D models are available for such cases that represent a vertical slice of aquifer. A full 3-D picture is only rarely available for a field site, and requires the use of numerous wells in the x–y plane screened at vertical intervals for discrete sampling. The classic studies performed at the Borden Landfill in Canada provide excellent examples of a well-monitored field test in 3-D (Mackay et al., 1986).

To study the variation in contaminants in 2-D, it is first necessary to solve the governing equations (Eq. (6.24) and (6.25)) in the x and y directions. The techniques available for developing a solution include analytical, semi-analytical, and sophisticated numerical methods that have been developed over the past 25 years. Analytical methods basically provide a closed form solution for relatively simple boundary and initial conditions. Semi-analytical methods usually result in an integral type solution that must be evaluated by a simple numerical integration procedure. Numerical methods are discussed in Chapters 8 and 10.

Analytical models are developed by solving the transport equation for certain simplified boundary and initial conditions. Numerous analytical solutions are available in the literature (Bear, 1979; Hunt, 1978; Wilson and Miller, 1978; Cleary and Ungs, 1978; Shen, 1976; Galya, 1987; Javandel et al., 1984; Domenico and Robbins, 1985) for pulse and continuous contaminant sources with boundary conditions ranging from no flow to constant heads. Processes that may be included in these models are advection, dispersion, adsorption, and first order decay (biological or radioactive). Analytical solutions generally require constant parameters, simple geometries, and well-defined boundary conditions, but they do provide useful insights into many ground water contaminant sites where two-dimensional variation can be assumed.

One of the first 2-D analytical models was that developed by Wilson and Miller (1978). It is one of the simplest to use and can account for lateral and transverse dispersion, adsorption, and first order decay in a uniform flow field. Concentration C at any point in the x,y plane can be predicted by solving Eq. (6.14) for an instantaneous spike source or for con-

tinuous injection. First order decay is added to the equation by adding a term, $-\lambda C$ to the left-hand side of Eq. (6.14), where the first order decay rate is λ [T^{-1}]. Velocity in the y-direction is assumed to be zero, and the x-axis is oriented in the direction of flow. Contaminants are assumed to be injected uniformly throughout the vertical axis.

Bear (1972) provides a solution to Eq. (6.14) for the condition where steady state conditions have been reached and the plume has been stabilized. The solution requires use of K_0, defined as the modified Bessel function of second kind and zero order. Q equals the rate at which a tracer of concentration C_0 is being injected.

$$C(x,y) = \frac{C_0 Q}{2\pi(D_x D_y)^{1/2}} \exp\left(\frac{v_x x}{2D_x}\right) K_0\left\{\frac{v_x^2}{4D_x}\left(\frac{x^2}{D_x}+\frac{y^2}{D_y}\right)^{1/2}\right\} \tag{6.26}$$

Case 6.5 Pulse Source Models. If a pulse of contaminant is injected over the full thickness of a two-dimensional homogeneous aquifer it will move in the direction of flow and spread out with time. Figure 6.6 represents the theoretical pattern of contamination at various points in time. A line source model from De Josselin De Jong (1958) assumes that the spill occurs as a line source (well) loaded vertically into a two-dimensional flow field (x, y). If a tracer with concentration C_0 is injected over an area A at a point (x_0, y_0), the concentration at any point (x, y) at time t after the injection is given by the following equation. Average linear velocity v_x, longitudinal dispersion, D_x, and transverse dispersion, D_y, are all assumed to be constant in this equation.

$$C(x,y,t) = \frac{C_0 A}{4\pi t(D_x D_y)^{1/2}} \exp\left\{-\frac{\left((x-x_0)-v_x t\right)^2}{4D_x t} - \frac{(y-y_0)^2}{4D_y t}\right\} \tag{6.27}$$

The corollary equation in 3-D from a point source was derived by Baetsle (1969) and can sometimes be used to represent the sudden release from a single source or tank in the subsurface. Baetsle's model gives the following equation:

$$C(x,y,z,t) = \frac{C_0 V_0}{8(\pi t)^{3/2}\left(D_x D_y D_z\right)^{1/2}} \exp\left[-\frac{(x-vt)^2}{4D_x t} - \frac{y^2}{4D_y t} - \frac{z^2}{4D_z t} - \lambda t\right] \tag{6.28}$$

where C_0 is the original concentration; V_0 is the original volume so that $C_0 V_0$ is the mass involved in the spill; D_x, D_y, D_z, are the coefficients of hydrodynamic dispersion; v is the velocity of the contaminant; λ is the first order decay constant for a radioactive substance. For a nonradioactive substance, the term λt is ignored.

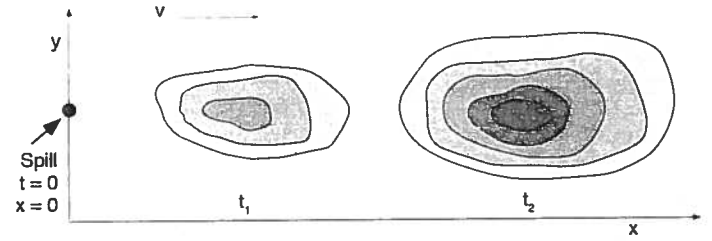

Figure 6.6 Plan view of instantaneous point source in time. Two dimensions.

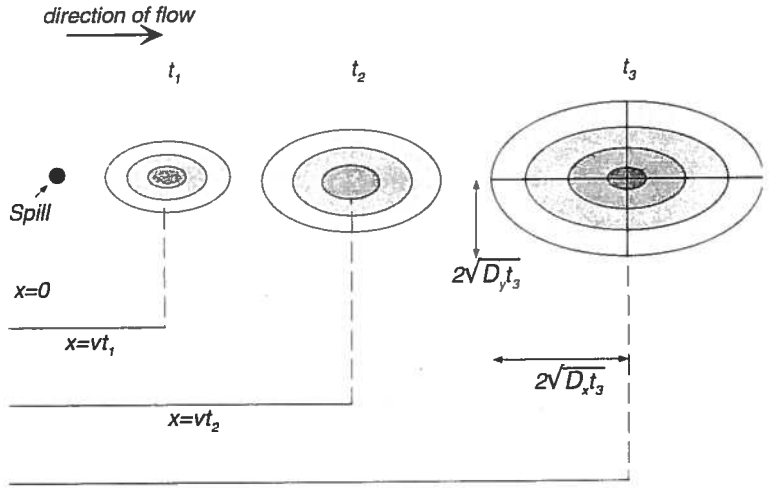

Figure 6.7 Plan view of plume developed from an instantaneous point source at three different times. Three dimensions.

With an idealized 3-D point source spill, spreading occurs in the direction of flow, and the peak or maximum concentration occurs at the center of the Gaussian plume where $y = z = 0$ and $x = vt$ (Figure 6.7).

$$C_{max} = \frac{C_0 V_0 e^{-\lambda t}}{8(\pi t)^{3/2}\left(D_x D_y D_z\right)^{1/2}} \tag{6.29}$$

The dimensions of the plume, assuming it actually started as a point source are

$$\sigma_x = (2D_x t)^{1/2}; \quad \sigma_y = (2D_y t)^{1/2}; \quad \sigma_z = (2D_z t)^{1/2} \tag{6.30}$$

where σ is the standard deviation, and $3\sigma_x$, $3\sigma_y$, and $3\sigma_z$ represent three standard deviations away from the mean within which 99.7% of the contaminant mass is contained.

EXAMPLE 6.2 TWO-DIMENSIONAL PULSE SOURCE.

A tank holding chloride at a concentration of 10,000 mg/L accidentally leaks over an area of 10 m^2 into an aquifer. Assuming that chloride is a completely conservative tracer, that D_x = 1 m^2/day and D_y = 0.1 m2/day, and that the seepage velocity is 1.0 m/day, calculate:

a) the time required for the center of mass of the plume to reach a point 75 m away;

b) the peak concentration at that point; and

c) the x and y dimensions of the plume at that point.

Solution.

a) Time required to reach 75 m:

$$t = \frac{R_f x}{V_w} = \frac{1\,(75\text{m})}{1\text{m/day}} = 75 \text{ days}$$

b) Peak concentration at 75 m:

$$C_{max} = \frac{C_0 A}{4\pi t (D_x D_y)^{1/2}}$$

$$= \frac{10^4 \text{mg/L} \times 10\text{m}^2}{4\pi \times 75 C_{max} \times (1\text{m}^2/\text{day} \times 0.1\text{m}^2/\text{day})^{1/2}}$$

$$= 335.7 \text{ mg/L}$$

c) Plume dimensions:

$\sigma_x = (2D_x t)^{1/2} = (2 \cdot 1 \cdot 75)^{1/2}$ m = 12.25 m

x dimension = $3\sigma_x$ = 36.7 m

$\sigma_y = (2D_y t)^{1/2} = (2 \cdot 0.1 \cdot 75)^{1/2}$ = 3.87 m

y dimension = $3\sigma_y$ = 11.6 m

6.8 MULTIDIMENSIONAL METHODS

Multidimensional methods include consideration of longitudinal, transverse, and vertical dispersion along with advection in one dimension. The governing Eq. (6.12) is altered to include only velocity in the x direction, and a first-order decay term can be added. Domenico and Robbins (1985) solved the problem analytically for the various source geometries shown in Figure 6.8. In their solution, they assume that the 3-D solution is made up of the product of three 1-D solutions. The source dimensions and dispersivities largely control the concentrations $C(x,y,z,t)$ that are predicted in the plume. The model can be applied in two dimensions by neglecting the z terms and adjusting the constant from 1/8 to 1/4. The Domenico analytical model is quite useful for screening purposes and for comparison to more complex numerical results at actual field sites. It has recently been applied for the biodegradation of chlorinated solvents (Newell et al., 1999). But care should be exercised since the results are very sensitive to the selection of the average width of the source zone. The model was developed for the case of a continuously leaking source, but through linear superposition of solutions lagged in time, a finite source (in time and space) can be represented as shown in the example below.

For the source geometry shown in Figure 6.8c, the resulting equation for $C(x,y,z,t)$ becomes

$$\frac{C(x,y,z,t)}{C_0} = \left(\frac{1}{8}\right) \text{erfc}\left[\frac{(x - vt)}{2(\alpha_x vt)^{1/2}}\right] \left\{\text{erf}\left[\frac{\left(y + \frac{Y}{2}\right)}{2(\alpha_y x)^{1/2}}\right] - \text{erf}\left[\frac{\left(y - \frac{Y}{2}\right)}{2(\alpha_y x)^{1/2}}\right]\right\} \left\{\text{erf}\left[\frac{(z + Z)}{2(\alpha_z x)^{1/2}}\right] - \text{erf}\left[\frac{(z - Z)}{2(\alpha_z x)^{1/2}}\right]\right\} \tag{6.31}$$

For the plane of symmetry $y = z = 0$, the above equation becomes

$$\frac{C(x,0,0,t)}{C_o} = \left(\frac{1}{2}\right) \text{erfc}\left[\frac{(x - vt)}{2(\alpha_x vt)^{1/2}}\right] \left\{\text{erf}\left[\frac{Y}{4(\alpha_y x)^{1/2}}\right] \text{erf}\left[\frac{Z}{4(\alpha_z x)^{1/2}}\right]\right\} \tag{6.32}$$

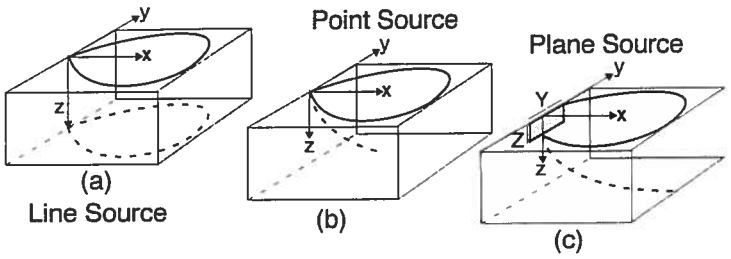

Figure 6.8 Geometrical considerations for a contaminant source. Shown in (a) is a vertical line source, in (b) a point source, and in (c) a finite plane source. Source: Domenico and Schwartz, 1998.

Note that when α_x and α_y approach zero, one obtains the original solution presented in Eq. (6.17) for the one-dimensional case.

Domenico (1987) presents the final form of the equation with first-order decay or degradation, which has the effect of a mass loss as the plume grows in space and time.

$$\frac{C(x,y,z,t)}{C_0} = \frac{1}{8}\exp\left\{\frac{x}{2\alpha_x}\left[1-\left(1+\frac{4\lambda\alpha_x}{v}\right)^{1/2}\right]\right\}\operatorname{erfc}\left[\frac{x-vt\left(1+4\lambda\alpha_x/v\right)^{1/2}}{2\left(\alpha_x vt\right)^{1/2}}\right]$$
$$\left\{\operatorname{erf}\left[\frac{\left(y+\frac{Y}{2}\right)}{2\left(\alpha_y x\right)^{1/2}}\right]-\operatorname{erf}\left[\frac{\left(y-\frac{Y}{2}\right)}{2\left(\alpha_y x\right)^{1/2}}\right]\right\}\left\{\operatorname{erf}\left[\frac{(z+Z)}{2\left(\alpha_z x\right)^{1/2}}\right]-\operatorname{erf}\left[\frac{(z-Z)}{2\left(\alpha_z x\right)^{1/2}}\right]\right\} \quad (6.33)$$

where λ, the decay constant, is 0.693 divided by the half-life.

EXAMPLE 6.3 APPLICATION OF THE MODEL TO A TRACER TEST.

There is a small dry cleaning facility with a PCE spill. A tracer test will be run at the site to enhance the understanding of hydraulic conditions. In order to design the test, develop a model using the Domenico and Robbins equations (Eqs. (6.31), (6.32), (6.33)) to simulate what should occur during the test. There are a total of six wells at the site; one injecting the tracer and five monitoring wells. Well diameter is 6 in. and the well screen fully extends into a 10 ft fine sand saturated zone. The tracer injected is 500 mg/L of bromide, injected at 3 gal/min. It is assumed that detection levels are down to the nearest 0.1 mg/L in the field.

Site characteristics:

- Aquifer is confined
- $K = 5 \times 10^{-3}$ cm/s
- The ground water gradient is 0.005
- Porosity is 0.3
- $\alpha_x = 0.5$ m, $\alpha_y = 0.1$ m
- 2-hr time step for testing

Solution. Taking into account the site and tracer characteristics and the placement of the five monitoring wells, model the breakthrough in the five wells. An Excel spreadsheet will greatly aid in the set-up and solving of this tracer problem. The model will be applied in 2-D by neglecting the z terms and adjusting the constant from 1/8 to 1/4 in Eq. (6.31). A one day pulse input can be modeled by superimposing a continuous input of C_0 and subtracting a negative input after one day. The resulting breakthrough curves can be plotted for each of the well locations. The results are clearly dependent on the selection of parameters in the model. Figure 6.9a shows the layout of the wells, Figure 6.9b shows the modeled concentrations of the tracer in the wells after a one day pulse, and Figure 6.9c shows the modeled concentrations for a continuous source. By observing concentrations from the tracer test and comparing to Figure 6.9b, one can determine or backout values for dispersivity in the x and y directions

Galya (1987) developed the horizontal plane source model (HPS). The model assumes 1-D velocity, but allows for 3-D dispersion in the x, y, and z directions. The governing equations are solved for a continuous release, although a finite source can be handled through linear superposition in time. The model's geometry is useful to analyze ponds or pits that leach contaminants from the surface down to the ground water table. The source term is treated in a unique way in order to maintain mass balances in the solution. This geometry is not as useful as the one used by Domenico above.

Another useful method, called the semi-analytical approach, has been developed by a number of researchers (Nelson, 1978; Bear, 1979). The method involves the computation of streamlines and equipotential lines over a flow domain via numerical integration. Javandel et al. (1984) showed how concentration versus time data for a single well can be mapped to other observation points to estimate spatial distribution in concentration. The computer program RESSQ calculates 2-D contaminant transport by advection and adsorption in a steady state flow field. Recharge wells and ponds act as sources and pumping wells act as sinks. RESSQ calculates streamline pattern in the aquifer, the location of contaminant fronts around sources at various times, and the variation of contaminant concentration with time at sinks. RESSQ was developed at the Lawrence Berkeley Laboratory based on a solution procedure by Gringarten and Sauty (1975). Javandel, et al. (1984) present a detailed discussion, listing, and users guide for the semi-analytical computer program RESSQ.

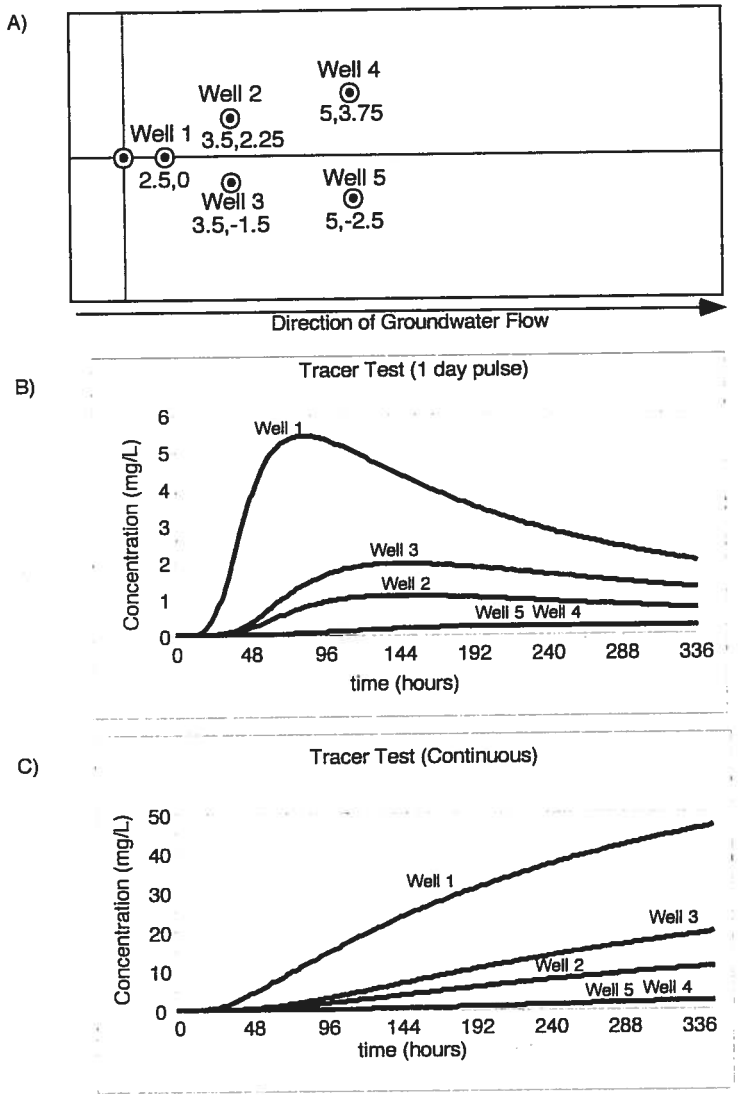

Figure 6.9 Site layout and tracer test plots (Example 6.3).

6.9 TESTS FOR DISPERSIVITY

To apply any 1-D or 2-D transport model properly to an actual site, it is first necessary to define the input parameters. For modeling a nonadsorbing solute such as chloride, the parameters of primary concern are water table elevation, hydraulic conductivity K, and dispersivity α. For small project sites, accurate delineation of the water table will depend on the number of wells that can be drilled. Porosity can easily be determined by laboratory testing of a few samples. While this limited sampling may result in errors in porosity of 10% to 20%, these errors will probably not be significant compared to the problems inherent in measuring hydraulic conductivity and dispersivity. Measurement of hydraulic conductivity was described in Chapters 3 and 5.

6.9.1 Laboratory Tests for Dispersivity

Soil column studies are often reported in terms of pore volumes where one pore volume represents the volume of water that completely will fill the voids along the column length. The total number of pore volumes U during a particular column test is the total discharge divided by a single pore volume.

$$U = \frac{v_x nAt}{ALn} = \frac{v_x t}{L} \tag{6.39}$$

where v_x = seepage velocity, A is the cross-sectional area, L is the length of the column, and n is porosity.

By rearranging Eq. (6.17) in terms of pore volumes and neglecting the second term on the right-hand side, one obtains a useful relation between C/C_0 and the pore volume function $(U-1)/U^{1/2}$. By plotting C/C_0 versus the pore volume function on normal probability paper, (Pickens and Grisak , 1981) demonstrated that data plot as a straight line, and the slope of the line is related to D_x, the longitudinal dispersion coefficient. The value of D_x can be found from

$$D_x = \frac{v_x L}{8}\left[J(0.84) - J(0.16)\right]^2 \tag{6.40}$$

where J(0.84) = the value of the pore volume function when $C/C_0 = 0.84$
and J(0.16) = the value of the pore volume function when $C/C_0 = 0.16$

because $D_x = \alpha_x v_x + D_d$

$$\alpha_x = \frac{D_x - D_d}{v_x} \tag{6.41}$$

Example 6.4 DISPERSION IN SAND COLUMNS

Pickens and Grisak (1981) studied dispersion in sand columns. They used sand with a mean grain size of 0.2 mm, porosity of 0.36 and uniformity coefficient of 2.3. The column had a length of 30 cm and diameter of 4.45 cm. Chloride (tracer) at a concentration of 200 mg/L was run through the column at a rate of 5.12×10^{-3} mL/s. Average linear velocity was 9.26×10^{-4} cm/s. The concentration of chloride in the effluent was measured as a function of U, and C/C_0 was plotted as a function of $[(U-1)/U^{1/2}]$ on probability paper as shown in Figure 6.10a.

At 25° C, the molecular diffusion coefficient for chloride in water is 2.03×10^{-5} cm²/s. From this, Pickens and Grisak estimated the effective diffusion coefficient to be 1.02×10^{-5} cm²/s. Hydrodynamic dispersion coefficients are based on the slope of the straight line. In the case of the above run, a hydrodynamic dispersivity of 4.05×10^{-5} cm²/s was obtained.

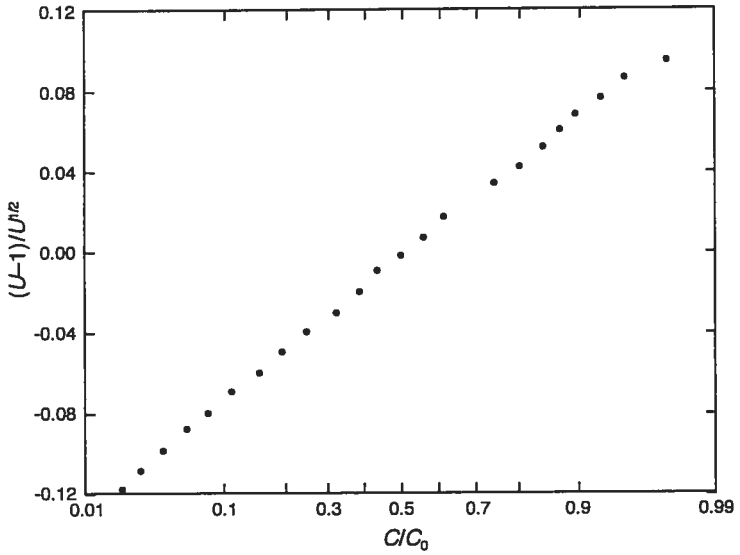

Figure 6.10a Plot of $(U-1)/U^{1/2}$ versus C/C_0 on probability paper for determination of dispersion in a laboratory sand column.

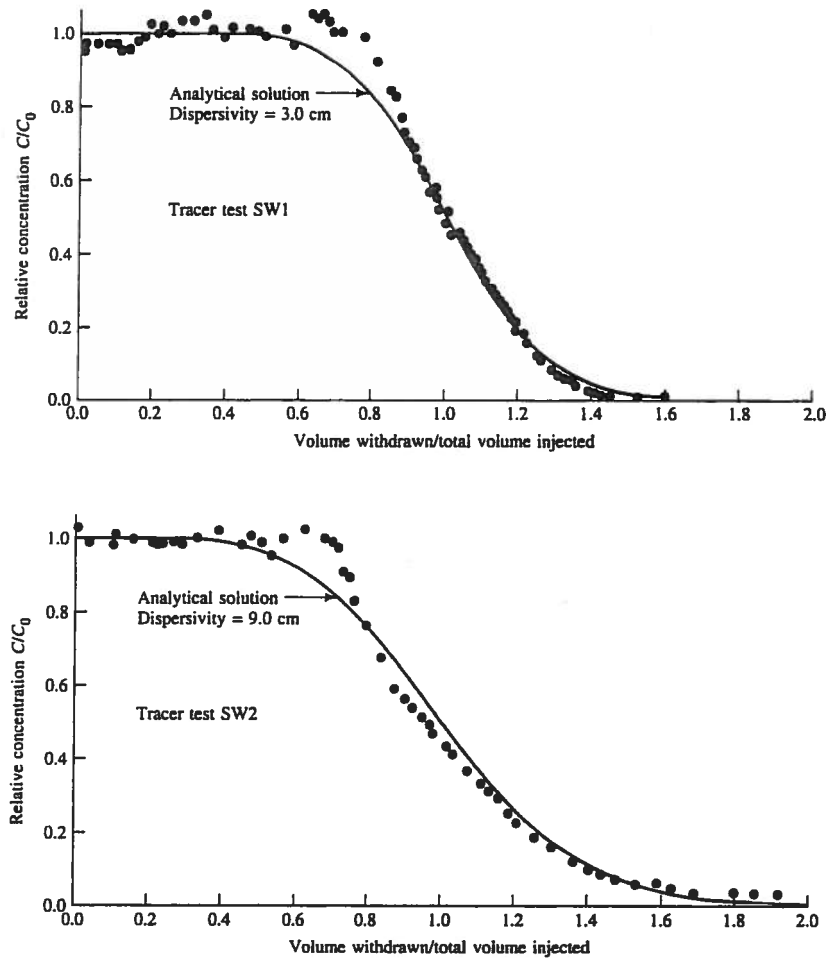

Figure 6.10b Comparison of measured C/C_0 values for a single well injection withdrawal test versus an analytical solution. Source: Pickens, 1981.

Finally, the dispersivity for the run was calculated using Eq. (6.41) as follows:

$$\alpha_x = \frac{D_x - D_d}{v_x}$$

$$= \frac{4.05 \times 10^{-5}\text{cm}^2/\text{sec} - 1.02 \times 10^{-5}\text{cm}^2/\text{sec}}{9.26 \times 10^{-4}\text{cm/sec}} = 0.033\text{cm}$$

6.9.2 Single Well Tracer Test

Pickens et al. (1981) report one of the very few field experiments for the *in situ* determination of dispersive and adsorptive properties of a well-defined sandy aquifer system. The aquifer was 8.2 m thick with $K = 1.4 \times 10^{-2}$ cm/s and porosity of 0.38. The technique involves the use of a radial injection dual-tracer test with ^{131}I as the nonreactive tracer and ^{85}Sr as the reactive tracer. Tracer migration was monitored at various radial distances and depths with multilevel point sampling devices. In the analysis of curves, nonequilibrium adsorption effects were incorporated into the dispersion terms of the solute transport equation rather than introducing a separate kinetic term.

Various curves were computed for different values of dispersivity and the curves were best fit to the field data collected at the well. Effective dispersivity values (α) obtained for ^{85}Sr ranged from 0.7 cm to 3.3 cm (mean of 1.9 cm), typically a factor of two to five times larger than those obtained for ^{131}I (range of 0.4 cm to 1.5 cm with a mean of 0.8 cm). The K_d values obtained by various analyses of the break-through curves ranged from 2.6 mL/g to 4.5 mL/g. These were within a factor of 4 of the mean values of K_d for ^{85}Sr based on a separate analysis of sediment cores in another part of the aquifer. The withdrawal phase for the well showed essentially full tracer recoveries for both compounds. The comparison of measured C/C_0 values for a single well tracer test versus an analytical solution is shown in Figure 6.10b. The two curves are based on longitudinal dispersivities of 3.0 cm and 9.0 cm, respectively. Thus, the usefulness of the dual-tracer injection tests has been demonstrated along with the existence of nonequilibrium conditions at a field site.

6.9.3 The Scale Effect of Dispersion

Dispersivity α is defined to be the characteristic mixing length and is a measure of the spreading of the contaminant. Unfortunately, this parameter has little physical significance and varies with the scale of the problem and sample method. Laboratory values range from 1 cm to 10 cm, while field studies often obtain values less than 1 m to over 1000 m.

Many investigators have recognized the scale effect of dispersion (Fried, 1975; Pickens and Grisak, 1981; Gelhar, 1986). A study by Gelhar et al. (1985) shows the scale dependency of longitudinal dispersivity at 55 actual field sites around the world (Figure 6.11). The data on the Gelhar graph from many sites around the world indicate a general increase in longitudinal dispersivity with scale, although the relation may not be linear. At the Borden landfill study described below (Mackay et al. 1986) determined that there was a small scale effect.

Since dispersion can be caused by slight differences in fluid velocity within a pore, or between pores, and because of different flow paths, the effect of different hydraulic conductivities in an aquifer can also cause spreading due to dispersion. The natural variation of hydraulic conductivity and porosity in a vertical and horizontal sense can play a key role in the scale effect of dispersion. As the flow path increases in length, ground water can encounter greater and greater variations in the aquifer. The deviations from the average increase along with the mechanical dispersion. It is logical to assume that dispersivity will approach some upper limit at long traveled distances and large travel times (Gelhar and Axness, 1983; Dagan, 1988). Due to a lack of field data, explanations of dispersion still represent an active research area.

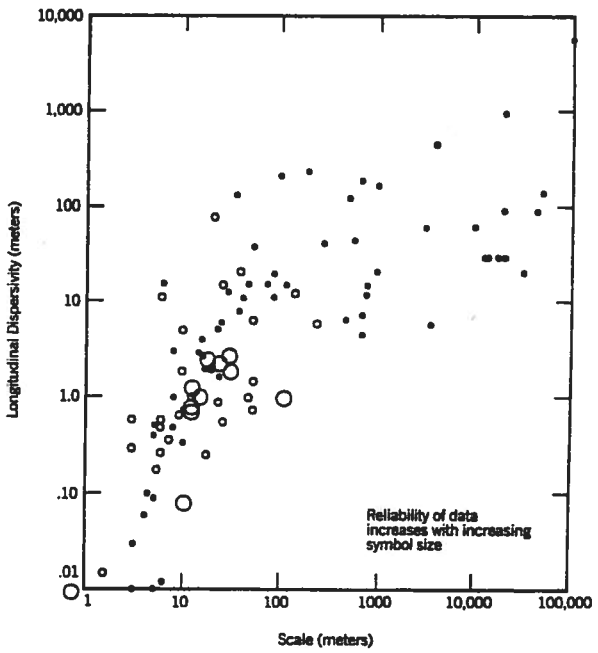

Figure 6.11 Scale of observation versus longitudinal dispersivity: reliability classification. Source: Gelhar, et al., 1985.

NATURAL GRADIENT FIELD TESTS FOR DISPERSION

6.10.1 Borden Landfill Natural Gradient Test

One of the most extensively monitored field tracer tests in history was performed by Cherry's research group at the Canadian Forces Base Borden (Sudicky et al. 1983; Mackay et al., 1986; Freyberg, 1986). An area near the landfill shown in Figure 6.12a was monitored extensively with multilevel sampling devices. The aquifer is about 20 m thick and thins to about 10 m in the direction of ground water flow, with an average hydraulic conductivity of 1.16×10^{-2} cm/s. In August 1982 a natural gradient field experiment was begun by injecting 12 m^3 into the subsurface of the sand aquifer. The average linear ground water velocity was computed to be 29.6 m/yr. The ground water flow direction is indicated in Figure 6.12a.

The concept was simply to inject a known amount of two conservative tracers and five volatile organic compounds for one day into a shallow, sand aquifer. Monitoring was continued for about two years at over 5000 observation points in 3-D (each well had up to 18 vertical screened intervals for sampling). Figure 6.12b shows the vertically averaged Cl^- distribution at four different times, and the various plumes were analyzed statistically by Freyberg (1986) in order to evaluate advection and dispersion in the natural gradient test. The mean ground water velocity was measured to be 0.091 m/day. It is clear from the gradual plume elongation depicted in Figure 6.12b that longitudinal dispersion was occurring and was much larger than transverse dispersion.

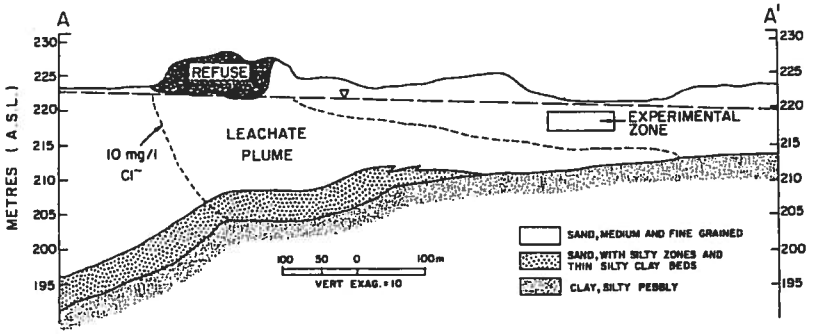

Figure 6.12a Approximate vertical geometry of aquifer along section AA'. Rectangle illustrates the vertical zone in which the experiment was conducted, which is above the landfill leachate plume (denoted by 10 mg/L chloride isopleth from 1979 data). Source: Mackay, et al., 1986.

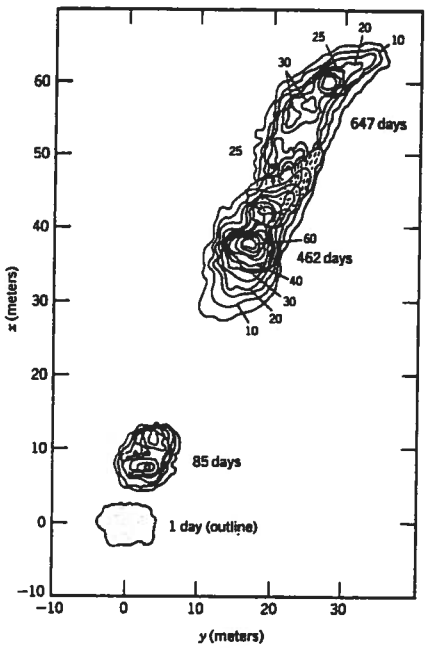

Figure 6.12b Vertically averaged concentration of distribution of Cl^- at various times after injection. Source: Mackay, et al., 1986.

Freyberg (1986) computed the center of mass of the chloride plume in 3-D as well as the variances in the longitudinal and transverse directions. The data was further analyzed by relating variance, time, and dispersivity. The dispersivities were first assumed to be constants with time, and then were shown to vary with time, indicating scale-dependent behavior. Freyberg (1986) calculated average linear values of α_x and α_y to be 0.36 m and 0.039 m, respectively, but indicated that α_x may be a function of time. Assuming scale-dependent behavior, a value of 0.43 m was computed, and was extrapolated to an asymptotic value of 0.49 m. Figure 6.12c shows the fit of the Borden data to a constant dispersivity model. The reader is referred to the complete set of six articles on the Borden natural gradient test in the December, 1986 issue of *Water Resources Research*.

Roberts et al. (1986) studied adsorption by analyzing arrival times of Cl^- compared to organics such as carbon tetrachloride at the wells at the Borden site. Chapter 7 describes the sorption results in more detail at the Borden site.

At an actual waste site, experimental determination of α_x and α_y is often impractical due to the very long flow times. In these cases, the most common approach is to run the transport model for a range of dispersivities and then adjust them until the predicted plume matches observed concentration data. Based on the Borden test data, a typical starting range for longitudinal dispersivity (α_x) in a sandy aquifer is 1 m to 10 m. Transverse dispersivity typically ranges from 10% to 30% of α_x. The procedure of fitting dispersivities to predict observed concentration patterns is admittedly crude but can lead to useful descriptions of contaminant transport.

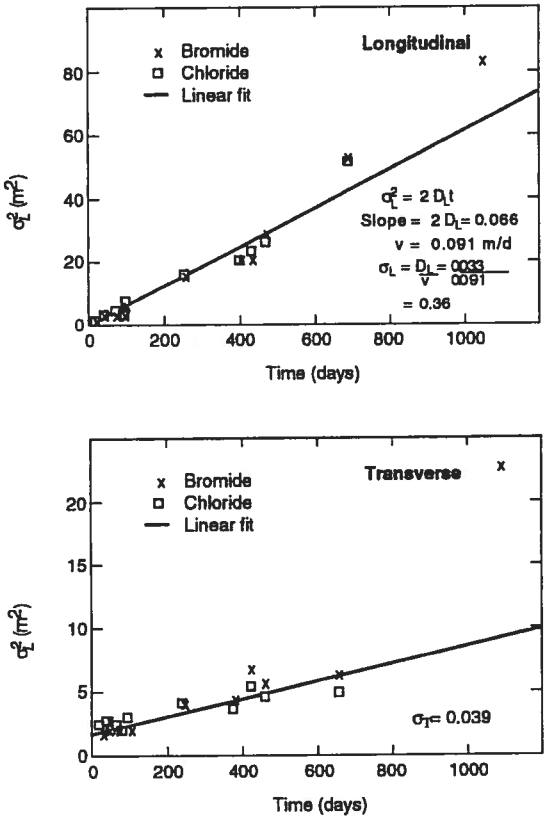

Figure 6.12c Fit of the Borden data to a constant dispersivity model. Source: Freyberg, 1986.

6.10.2 Natural Gradient Tracer Test, Cape Cod, Mass.

This natural gradient tracer experiment was designed to provide a well-defined set of initial conditions associated with contaminant release. An extensive and systematic monitoring program was undertaken so that a detailed description of the resulting contaminant plume could be established and maintained over an extended period of time as it moved and dispersed within the aquifer. The collected data was then used to evaluate the validity of currently accepted theories used to predict solute movement and behavior in the saturated zone. Results were compared to those that were found at the Borden Landfill Experiment.

Description of the Site and Experiment. The site of the experiment was a sand and gravel aquifer located on Cape Cod, Massachusetts (Figure 6.13) near Otis Air Base.

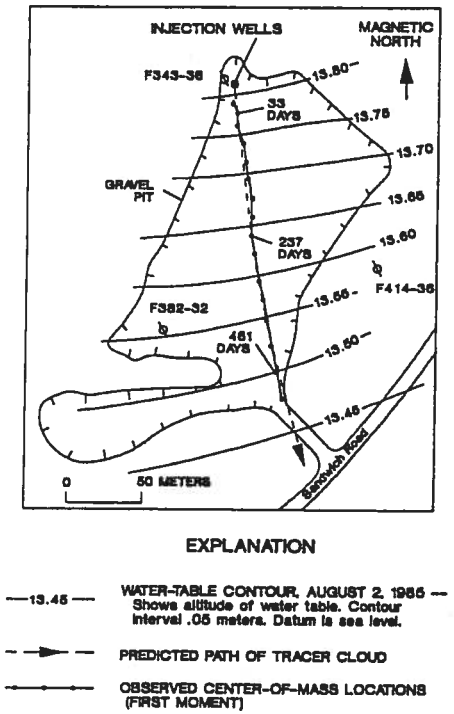

Figure 6.13 Horizontal trajectory of the center of mass of the bromide plume at the Cape Cod site. Source: Garabedian et al., 1991.

The nature of the site and the experiment was originally described by LeBlanc et al. (1991). The site was composed of approximately 100 m of unconsolidated sediments that overlay an impermeable bedrock stratum. The upper 30 m of the site consisted of horizontally stratified sand and gravel deposits. Beneath these deposits the sediments consisted of fine-grained sand and silt. These deposits formed an unconfined aquifer with a mean water table elevation located approximately 5 m beneath the ground surface. Several small-scale tracer tests that were conducted at the site revealed an overall effective porosity of 0.39. The magnitude of the horizontal hydraulic gradient was found to vary from 0.0014 to 0.0018 while a vertical gradient was nondetectable. The average hydraulic conductivity was estimated from an in situ flow test to be 110 m/d. More detailed analyses conducted with a borehole flow meter in conjunction with permeameter testing of core samples showed the hydraulic conductivity to vary by about one order of magnitude across the site due to the interbedded lens structure of the aquifer. Based on the values quoted above for effective porosity, hydraulic gradient, and hydraulic conductivity the mean ground water velocity at the site was calculated to be 0.4 m/d.

Solute injection at the Cape Cod site was accomplished by the placement of 7.6 m^3 of tracer solution into the saturated zone through three injection wells at the rate of 7.6 L/min (2.5 L/min/well). This slow injection rate was selected in order to minimize spreading of the plume during injection. Both nonreactive and reactive tracers were used. Bromide was selected as the nonreactive tracer due to the fact that chloride was present at relatively high natural concentrations in the aquifer. The reactive tracers used were lithium, molybdate, and fluoride. A summary of the solution composition is presented in Table 6.2.

The sampling array was composed of 656 multilevel samplers. All total there were 9,840 individual sampling points at the site. The focus of sample collection was on obtaining synoptic ("snapshot") data, thus sampling episodes took place on roughly monthly intervals over a three year period (1985-1988). The data collected at the site included approximately 30,000 bromide analyses, 33,000 lithium analyses, and 38,000 molybdate analyses. Fluoride was abandoned as a tracer early in the test due to the fact that it was so strongly sorbed that trace concentrations remaining in solution became indistinguishable from background levels. Figure 6.14 shows the sampling layout.

Overview of Plume Behavior. Significant features of the resulting contaminant cloud observed at the Cape Cod site include a predominant spreading in the direction of ground water flow, minimal spreading in the horizontal transverse direction, and essentially no spreading in the vertical direction. These features combined to create a narrow plume that was aligned in the direction of ground water flow. Figure 6.15 provides a comparison of the

TABLE 6.2 Injected Solutes at the Cape Cod Site

Solute	Injected Concentration (mg/L)	Injected Mass (g)	Background Concentration (mg/L)
Bromide	640	4900	<0.10
Lithium	78	590	<0.01
Molybdate	80	610	<0.02
Fluoride	50	380	<0.20

From LeBlanc et al., 1991.

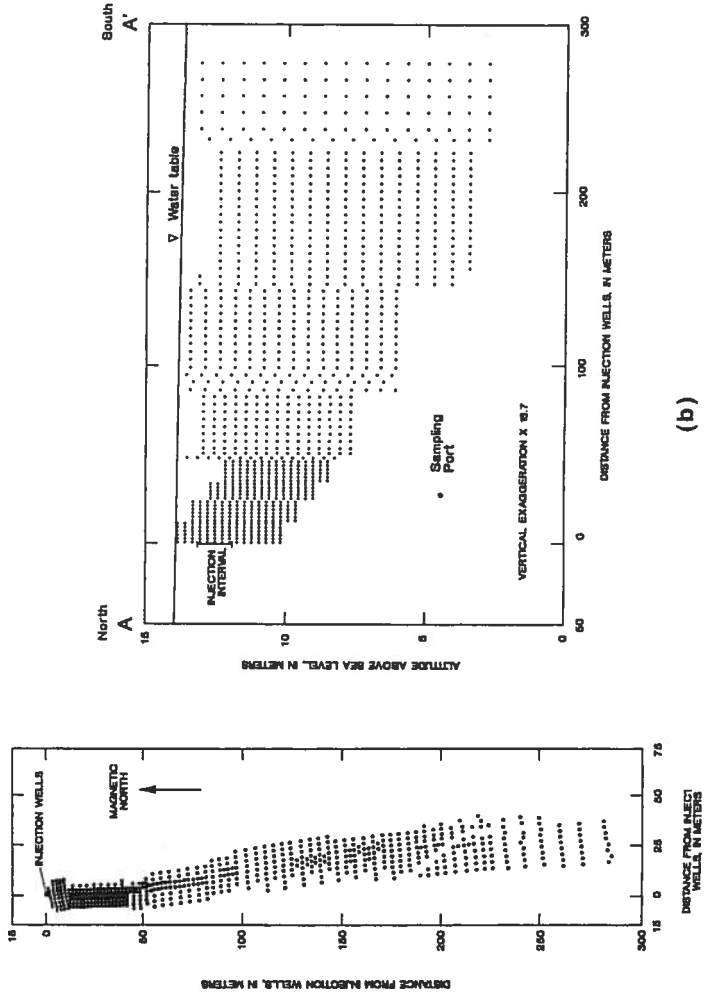

Figure 6.14 Locations of multilevel samplers and injection wells at the Cape Cod Site. (a) Plan view. (b) Vertical distribution of sampling points along representative section. Source: LeBlanc et al., 1991. © American Geophysical Union.

bromide, lithium, and molybdate plumes at various times following injection. Note that the movement of the reactive species, lithium and molybdate, is significantly retarded in comparison with the conservative bromide.

Inspection of the vertical concentration profiles for bromide recorded at the site reveals minimal vertical spreading. However, also of interest is the downward movement of the plume with horizontal travel distance (Figure 6.14b). This vertical movement was attributed to two effects: (1) vertical flow associated with areal recharge and (2) sinking of the plume due to density differences between the tracer solution and the natural ground water (LeBlanc et al., 1991).

Experimental Observations. As a conservative tracer, the total mass of bromide in solution should be constant with time and should be equal to the mass injected. Evaluation of the mass of bromide contained in each plume for each of 16 separate synoptic data sets yielded the plot of total mass versus time data. The trend of effectively constant mass over time may be inferred. The differences between the calculated mass and the injected mass may be attributed to measurement and estimation error (Garabedian et al., 1991).

A graphical representation of the horizontal trajectory of the center of mass of the tracer plume is given in Figure 6.13. The movement of the center of mass is quite linear and closely corresponds to the direction predicted by the water table gradient. While some vertical displacement of the center of mass was observed, as noted above, this movement was considered inconsequential by the researchers in comparison with the large horizontal displacement and so a strictly horizontal transport velocity could be assumed. The observed ground water flow velocity at the site as given by the slope of the line fitted through this data was computed as 0.42 m/d. This value is consistent with that calculated using the average measured porosity, hydraulic gradient, and hydraulic conductivity.

A theoretical approach to describing dispersivity in the ground water environment as a function of time has been developed by Dagan (1982, 1984). Dagan's theory suggests that limiting values of dispersivity will be reached for large values of time. Typically this large time value corresponds to a plume that has reached a scale of spreading that is significantly larger than the scale of hydraulic conductivity variability (Garabedian et al., 1991).

In order to study this idea of an asymptotic dispersivity the Cape Cod study was designed to incorporate a large (280 m) plume travel distance. Data from the experiment showed a constant value of longitudinal dispersivity, develop after a short period of nonlinear growth. The data also indicated a positive valued transverse dispersivity that was constant with time. The horizontal and transverse dispersivity values were determined to be 0.96 m and 0.018 m respectively. The vertical dispersivity was calculated to be 0.0015 m. While the asymptotic nature of the longitudinal dispersivity was clear, the nonzero value of transverse dispersivity was not in agreement with the theory of Dagan (1984). One may note from these results, however, that the typical assumption that the longitudinal dispersivity is an order of magnitude larger than the transverse dispersivity was supported by the data.

In order to study this idea of an asymptotic dispersivity the Cape Cod study was designed to incorporate a large (280 m) plume travel distance. Data from the experiment showed a constant value of longitudinal dispersivity develop after a short period of non-linear

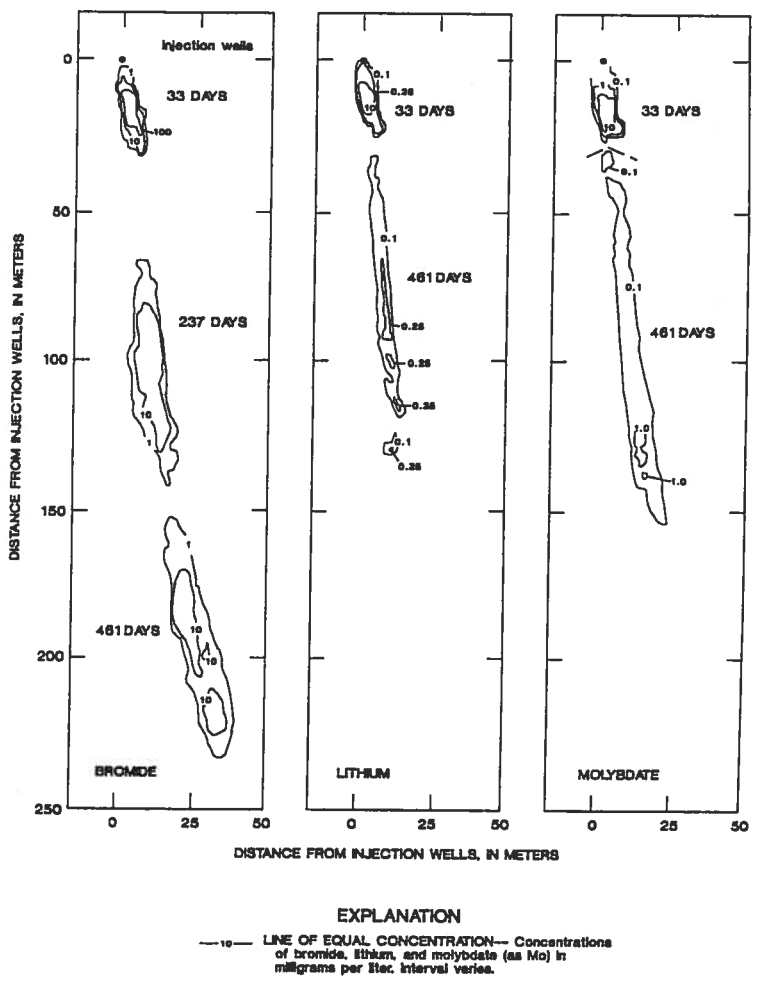

Figure 6.15 Vertical location of bromide plume at 33, 237, and 461 days after injection at the Cape Cod site. Source: LaBlanc, 1991.

growth. The data also indicated a positive valued transverse dispersivity that was constant with time. The horizontal and transverse dispersivity values were determined to be 0.96 m and 0.018 m respectively. The vertical dispersivity was calculated to be 0.0015 m. While the asymptotic nature of the longitudinal dispersivity was clear, the non-zero value of transverse dispersivity was not in agreement with the theory of Dagan (1984). One may note from these results, however, that the typical assumption that the longitudinal dispersivity is an order of magnitude larger than the transverse dispersivity was supported by the data.

Significant Findings and Comparisons. A large scale natural gradient tracer experiment was performed in a shallow, unconfined, sand and gravel aquifer. The purpose of this experiment was to assess the validity of the often-made simplifying assumptions used in the application of theoretical transport models to field situations where extensive data is not available. There were similarities between the results of the two tests at Borden and Cape Cod which include:

1. The advective velocity and trajectory of a solute can be adequately predicted using conventionally collected data (i.e., porosity, hydraulic gradient, and hydraulic conductivity estimated from any of several techniques).
2. The relative magnitudes of dispersion follow the trend of longitudinal dispersion > transverse dispersion > vertical dispersion and that transverse dispersion is an order of magnitude less than longitudinal dispersion.
3. A limiting value of dispersivity is reached at large values of time (travel distance) after an early period of nonlinear growth.
4. A retardation mechanism function to limit the movement of reactive solutes relative to nonreactive solutes.

Differences between the two tests indicate a much greater hydraulic conductivity and seepage velocity at Cape Cod (0.42 m/day) versus Borden (0.091 m/day). Longitudinal dispersivity was 0.96 m at Cape Cod versus 0.43 m at Borden, and the ratio of longitudinal to transverse dispersivity was much greater at Cape Cod (50 to 1) than at Borden (11 to 1). Garabedian et al. (1991) present more details on the comparison of the two tests.

IMARY

Basic concepts in ground water transport processes include problems in one, two, and three dimensions with advection, dispersion, adsorption, and biodegradation. The 1-D solutions to the advective dispersion equation allow simple predictions of breakthrough with adsorption or decay. Analytical expressions allow reasonable estimates for travel time and spreading of contaminant fronts in 1-D soil columns. Two-dimensional models can be solved analytically for simple boundary conditions, but numerical models are generally required for actual field problems. Multidimensional methods such as the Domenico model and the HPS model can provide useful estimates of concentrations from simple planar source areas. These models provide some idea of concentrations in time and space from continuously leaking source areas with a constant velocity flow field and simple boundary conditions. Other models such as RESSQ can be used to calculate steady-state streamline patterns and contaminant transport in the presence of recharge wells and ponds.

Tests for dispersivity in the laboratory and in the field are reviewed. There are many problems associated with parameter estimation at field sites, including estimation of hydraulic conductivity, dispersivity, and adsorption coefficients. Extrapolation of results from laboratory column experiments to field sites has proven to be quite difficult, and therefore methods that can be directly applied to the field are being developed by researchers. Results from the extensive natural gradient tracer studies performed at the Borden landfill in Canada and at the Cape Cod, Mass. are briefly described. These two sites represent the most comprehensive databases on advective-dispersive transport that are available in the general literature.

REFERENCES

Anderson, M. P., "Using Models To Simulate The Movement Of Contaminants Through Ground Water Flow Systems," *CRC Critical Rev. Environ. Control*, Chemical Rubber Co., 9, 96, 1979.

Anderson, M. P. and W. W. Woessner, *Applied Ground Water Modeling*, San Diego, CA, Academic Press, Inc, 1992.

Barker, J. F., G. C. Patrick, and D. Major, "Natural Attenuation of Aromatic Hydrocarbons in a Shallow Sand Aquifer," *Ground Water Mon. Rev.*, p. 64-71, 1987.

Bear, J. *Dynamics of Fluids in Porous Media*. New York: American Elsevier Publishing Company, 764 pp., 1972.

Bear, J., *Hydraulics of Ground Water*, New York, NY, McGraw-Hill, 1979.

Borden, R. C. and P. B. Bedient, "Transport Of Dissolved Hydrocarbons Influenced By Reaeration And Oxygen Limited Biodegradation: 1. Theoretical Development," *Water Resources Res.* 22:1973-1982, 1986.

Bredehoeft, J. D. and G. F. Pinder, "Mass Transport in Flowing Ground Water," *Water Resources Res.* 9, 192-210, 1973.

Charbeneau, R. J., "Ground Water Contaminant Transport With Adsorption And Ion Exchange Chemistry: Method Of Characteristics For The Case Without Dispersion, *Water Resources Res.*, 17:3:705-713, 1981.

Charbeneau, R. J., "Calculation Of Pollutant Removal During Ground Water Restoration With Adsorption And Ion Exchange, *Water Resources Res.*, 18:4:1117-1125, 1982.

Cleary, R. W. and M. J. Ungs, "Ground Water Pollution and Hydrology, Mathematical Models and Computer Programs," *Rep. 78-WR-15*, Water Resour. Program, Princeton, N.J., Princeton Univ., 1978.

Dagan, G., "Stochastic Modeling Of Ground Water Flow By Unconditional And Conditional Probabilities, 2, The Solute Transport," *Water Resources Res., 18(4)*, 835-848, 1982.

Dagan, G., "Solute Transport In Heterogeneous Porous Formations," *J. Fluid Mech., 145*, 151-177, 1984.

ıgan, G. "Statistical Theory of Ground Water Flow and Transport: Pore to Laboratory, Laboratory to Formation, and Formation to Regional Scale," *Water Resources Res.*, 22, no. 9:120S-134S, 1986.

ıgan, G., "Theory of Solute Transport in Water," *Annual Reviews of Fluid Mechanics*, 19:183-215, 1987.

ıgan, G. "Time-dependent Macrodispersion for Solute Transport in Anisotropic Heterogeneous Aquifers," *Water Resources Res.*, 24, no. 9:1491-1500, 1988.

ɜ Josselin De Jong, G., "Longitudinal and Transverse Diffusion in Granular Deposits. Transactions," American Geophysical Union 39, no. 1:67, 1958.

ɔmenico, P. A. and G. A. Robbins, "A New Method of Contaminant Plume Analysis," *Ground Water*, vol. 23, pp. 476-485, 1985.

ɔmenico, P. A. and F. W. Schwartz, *Physical and Chemical Hydrogeology*, New York, John S. Wiley and Sons, 1990.

omenico, P. A. and F. W. Schwartz, *Physical and Chemical Hydrogeology*, 2nd Edition, New York, NY, John S. Wiley and Sons, 1998.

'eeze, R. A. and J. A. Cherry, *Ground Water*, Englewood Cliffs, NJ, Prentice-Hall, 1979.

'eyberg, D. L., "A Natural Gradient Experiment On Solute Transport In A Sand Aquifer, (2) Spatial Moments And The Advection And Dispersion Of Nonreactive Tracers," *Water Resources Res.*, 22:13: 2031-2046, 1986.

ried, J. J., *Ground Water Pollution*. Amsterdam, Elsevier, 1975.

alya, D. P., "A Horizontal Plane Source Model for Ground-Water Transport," *Ground Water*, Vol. 25, No. 6, 1987.

arabedian, S. P., D. R. LeBlanc, L. W. Gelhar, and M. A. Celia, "Large-Scale Natural Gradient Tracer Test In Sand And Gravel, Cape Cod, Massachusetts, 2, Analysis Of Spatial Moments For A Nonreactive Tracer," *Water Resources Res., 27(5)*, 911-924, 1991.

elhar, L. W. and C. L. Axness, "Three-dimensional Stochastic Analysis of Macrodispersion in Aquifers," *Water Resources Res.*, 19, no. 1:161-80, 1983.

elhar, L.W., A.L. Gutjahr, and R.L. Naff, "Stochastic Analysis Of Macrodispersion In A Stratified Aquifer," *Water Resources Res.*, 15:6:1387-1397, 1979.

elhar, L.W., A. Montoglou, C. Welty, and K.R. Rehfeldt, "A Review Of Field-Scale Physical Solute Transport Processes In Saturated And Unsaturated Porous Media," *Final Proj. Rep. EPRI EA-4190*, Palo Alto, CA,, Elec. Power Res. Inst., 1985.

elhar, L. W., "Stochastic Subsurface Hydrology from Theory to Applications," *Water Resources Res.*, 22, no. 9:135S-145S, 1986.

ringarten, A. C. and J. P. Sauty, "A Theoretical Study of Heat Extraction from Aquifers with Uniform Regional Flow," *J. Geophys. Res.*, 80(35), 4956-4962, 1975.

lunt, B., "Dispersive Sources in Uniform Ground-Water Flow," *J. Hydraulics Div.* ASCE 104:75-85, 1978.

avandel, I., C. Doughty, and C.F. Tsang, *Ground Water Transport: Handbook of Mathematical Models*, American Geophysical Union, Water Resources Monograph 10, Washington, DC, 228 pp., 1984.

eBlanc, D. R., S. P. Garabedian, K. M. Hess, L. W. Gelhar, R. D. Quadri, K. G. Stollenwerk, and W. W. Wood, "Large-Scale Natural Gradient Tracer Test In Sand And Gravel, Cape Cod, Massachusetts, 1, Experimental Design And Observed Tracer Movement," *Water Resources Res., 27(5)*, 895-910, 1991.

Mackay, D.M., D.L. Freyberg, P.V. Roberts, and J.A. Cherry, "A Natural Gradient Experiment On Solute Transport In A Sand Aquifer, (1) Approach And Overview Of Plume Movement," *Water Resources Res.*, 22:13:2017-2029, December 1986.

Mercer, J. W. and C. R. Faust, 1981, *Ground-Water Modeling*, NWWA, 2nd Ed., 1986.

Nelson, R. W., "Evaluating the Environmental Consequences of Groundwater Contamination. 1. An Overview of Contaminant Arrival Distributions as General Evaluation Requirements," *Water Resources Res.*, 14:409-515, 1977.

Neuman, S. P., C. L. Winter, and C. N. Newman, "Stochastic Theory Of Field-Scale Fickian Dispersion In Anisotropic Porous Media," *Water Resources Research* 23, no. 3:453-66, 1987.

Newell, C J., Gonzales, J., and McLeod, R., *BIOSCREEN Natural Attenuation Decision Support System, Version 1.4* Revisions, U.S. Environmental Protection Agency, 1999.

Ogata, A., "Theory Of Dispersion In A Granular Medium," U.S. Geological Survey Professional Paper 411-I, 1970.

Pickens, J. F. and G. E. Grisak., "Scale-dependent Dispersion in a Stratified Granular Aquifer," *Water Resources Research* 17, no. 4:1191-1211, 1981.

Pickens, J. F., R. E. Jackson, K. J. Inch, and W. F. Merritt, "Measurement Of Distribution Coefficients Using A Radial Injection Duel-Tracer Test," *Water Resources Res.* 17, no. 3:529-44, 1981.

Rifai, H. S., P. B. Bedient, J. T. Wilson, K. M. Miller, and J. M. Armstrong, "Biodegradation Modeling At A Jet Fuel Spill Site," ASCE *J. Environmental Engr. Div.* 114:1007-1019, 1988.

Roberts, P.V., M.N. Goltz, and D.M. Mackay, "A Natural Gradient Experiment On Solute Transport In A Sand Aquifer, (4), Sorption Of Organic Solutes And Its Influence On Mobility," *Water Resources Res.*, 22:13:2047-2058, December 1986.

Shen, H.T., "Transient Dispersion in Uniform Porous Media Flow," *J. Hydrau. Div.* ASCE 102:707-716, 1976.

Smith, L., and F. W. Schwartz, "Mass Transport: 1. A Stochastic Analysis of Macroscopic Dispersion," *Water Resources Res.* 16:303-313, 1980.

Sudicky, E. A., J. A. Cherry, and E. O. Frind. "Migration of Contaminants in Ground Water at a Landfill: A Case Study, 4, A Natural Gradient Dispersion Test." *Journal of Hydrology* 63, no. 1/2:81-108, 1983.

Wang, H.F. and M.P. Anderson, *Introduction to Ground Water Modeling, Finite Difference and Finite Element Methods*, San Francisco, CA, W.H. Freeman and Company, 237 pp., 1982.

Wilson, J. L., Miller, P.J., "Two-Dimensional Plume in Uniform Ground Water Flow," *J. Hydrau. Div.* ASCE 104:503-514, 1978.

Zheng, C. and G. D. Bennett, *Applied Contaminant Transport Modeling: Theory and Practice*, New York, NY, Van Nostrand Reinhold, 1995.